Error Estimator for Cauer Ladder Network Representation

Shingo Hiruma[1], Stéphane Clénet[2], Hajime Igarashi[3], and Thomas Henneron[2]

[1]Graduate School of Engineering, Kyoto University, Kyoto 615-8510, Japan
[2]Université de Lille, Arts et Metiers Institute of Technology, Centrale Lille, Junia, ULR 2697 - L2EP, F-59000 Lille, France
[3]Graduate School of Information Science and Technology, Hokkaido University, Sapporo 060-0814, Japan

The Cauer Ladder Network (CLN) method enables to construct a reduced based circuit model of analytical or numerical models, e.g. Finite Element (FE) model, under quasistatic approximation. This paper proposes an estimator which provides guaranteed upper bounds of the truncation error due to the CLN method. The error estimator is tested on an analytical model and a Finite Element model to validate the approach.

***Index Terms*— Cauer ladder network (CLN), error estimation, Maxwell's equations, model order reduction (MOR).**

I. Introduction

Model order reduction has been gaining attention because it can drastically reduce the number of unknowns of a problem with little loss of accuracy. Recently, the Cauer Ladder Network (CLN) method [1] has been proposed by Kameari, et al. Using the CLN method, an equivalent electrical circuit can be extracted from analytical or numerical models, e.g. Finite Element (FE) model, under quasistatic approximation. A new entry of basis is calculated at each iteration, and the reduced solution is sought in the basis. The truncation error, i.e. error between the reduced and the exact solution of the problem, decreases with the iteration number. In most cases, however, we do not know a priori the iteration number leading to an accurate reduced solution versus the exact solution. The issue is then to find the trade-off between limiting the iteration number while controlling the truncation error.

In this study, we propose an estimator of the truncation error introduced by the CLN method in the case of magnetoharmonic problem. Like in numerical error estimation theory [2], the error estimator is based on a relationship between the solution of the reduced model and the exact solution. The error estimator is tested on an analytical model and an FE model to validate the approach.

II. Methodology

A. Introduction of the error estimator

Let us consider a magnetoharmonic problem on a domain Ω governed by the following equations:

$$\mathrm{curl}\boldsymbol{E} = -j\omega\mu\boldsymbol{H}, \tag{1}$$
$$\mathrm{curl}\boldsymbol{H} = \sigma\boldsymbol{E}, \tag{2}$$

with $\boldsymbol{H}$ the magnetic field, $\boldsymbol{E}$ the electric field, σ the conductivity, μ the permeability, j the imaginary unit, and ω the angular frequency. $\boldsymbol{E}$ and $\boldsymbol{H}$ have also to satisfy boundary conditions on $\partial\Omega$. If we consider a triplet $(\boldsymbol{H}, \boldsymbol{H}', \boldsymbol{E})$ such that $(\boldsymbol{H}, \boldsymbol{E})$ and $(\boldsymbol{H}', \boldsymbol{E})$ satisfy (1) and (2), respectively, we can show that (see Appendix A):

$$\epsilon_h^2 = \|\boldsymbol{H}' - \boldsymbol{H}\|_\mu^2 = \|\boldsymbol{H}' - \boldsymbol{H}_{\mathrm{ex}}\|_\mu^2 + \|\boldsymbol{H}_{\mathrm{ex}} - \boldsymbol{H}\|_\mu^2, \tag{3}$$

with $\|\boldsymbol{X}\|_\mu^2 = \int_\Omega \boldsymbol{X}^* \cdot \mu\boldsymbol{X} d\Omega$ the energy norm where $*$ is the conjugate operator, and $\boldsymbol{H}_{\mathrm{ex}}$ the exact solution of the magnetoharmonic problem, which means Pythagorean's theorem holds for the two residual vectors $\boldsymbol{H}' - \boldsymbol{H}_{\mathrm{ex}}$ and $\boldsymbol{H}_{\mathrm{ex}} - \boldsymbol{H}$. Similarly, if we consider a triplet $(\boldsymbol{H}, \boldsymbol{E}, \boldsymbol{E}')$ such that $(\boldsymbol{H}, \boldsymbol{E})$ and $(\boldsymbol{H}, \boldsymbol{E}')$ satisfy (2) and (1), respectively, we can show that:

$$\epsilon_e^2 = \|\boldsymbol{E}' - \boldsymbol{E}\|_\sigma^2 = \|\boldsymbol{E}' - \boldsymbol{E}_{\mathrm{ex}}\|_\sigma^2 + \|\boldsymbol{E}_{\mathrm{ex}} - \boldsymbol{E}\|_\sigma^2, \tag{4}$$

with $\|\boldsymbol{X}\|_\sigma^2 = \int_\Omega \boldsymbol{X}^* \cdot \sigma\boldsymbol{X} d\Omega$ the energy norm and $\boldsymbol{E}_{\mathrm{ex}}$ the exact solution of the magnetoharmonic problem. Based on this property, we propose to construct an error estimator for the CLN approximation.

B. Error estimator for CLN

We approximate the solution of the magnetoharmonic problem coupled with an external circuit by a N-stage Cauer circuit with a resistive termination (see Fig.1). We obtain then an equivalent circuit approximating the response of the system. This equivalent circuit is obtained after N iterations of the CLN method as well as the approximations of $\boldsymbol{E}^N$ and $\boldsymbol{H}^N$ given by [1]:

$$\boldsymbol{E}^N = \sum_{n=0}^{N} v_{2n}\boldsymbol{E}_{2n}, \qquad \boldsymbol{H}^N = \sum_{n=0}^{N-1} i_{2n+1}\boldsymbol{H}_{2n+1}, \tag{5}$$

with the voltages $v_0, v_2, \ldots, v_{2N}$ and the currents $i_1, i_3, \ldots, i_{2N-1}$ obtained after solving the circuit equations (see Fig.1) and the basis $\boldsymbol{E}_0, \boldsymbol{E}_2, \ldots, \boldsymbol{E}_{2N}, \boldsymbol{H}_1, \boldsymbol{H}_3, \ldots, \boldsymbol{H}_{2N-1}$ obtained by the CLN method. The fields $\boldsymbol{E}^N$ and $\boldsymbol{H}^N$ tend to the exact solutions $\boldsymbol{E}_{\mathrm{ex}}$ and $\boldsymbol{H}_{\mathrm{ex}}$ of the magnetoharmonic problem when N tends to infinity. The issue is then to choose the size N of the expansion, which enables to get the desired accuracy of the approximation given by (5) in terms of the energy norm $\|\cdot\|_\mu^2$. In order to estimate the error, we define an additional field $\boldsymbol{H}'^N$:

$$\boldsymbol{H}'^N = \boldsymbol{H}^N + i_{2N+1}\boldsymbol{H}_{2N+1}, \tag{6}$$

where i_{2N+1} is the current flowing through the termination resistor of the Cauer circuit and given by $i_{2N+1} = \frac{v_{2N}}{R_{2N}}$ (Fig.1). We can show that the couples $(\boldsymbol{H}^N, \boldsymbol{E}^N)$ and $(\boldsymbol{H}'^N, \boldsymbol{E}^N)$ satisfy (1) and (2), respectively (see Appendix B). Thus, we obtain the error estimator ϵ_h^2 by applying (3):

$$\begin{aligned} \epsilon_h^2 &= \|\boldsymbol{H}'^N - \boldsymbol{H}^N\|_\mu^2 \\ &= \|i_{2N+1}\boldsymbol{H}_{2N+1}\|_\mu^2 \\ &= L_{2N+1}|i_{2N+1}|^2 \\ &= \|\boldsymbol{H}'^N - \boldsymbol{H}_{\text{ex}}\|_\mu^2 + \|\boldsymbol{H}_{\text{ex}} - \boldsymbol{H}^N\|_\mu^2 \\ &\geq \|\boldsymbol{H}_{\text{ex}} - \boldsymbol{H}^N\|_\mu^2. \end{aligned} \tag{7}$$

The term ϵ_h^2 is an upper bound of the distance between the field $\boldsymbol{H}^N$ given by the CLN method and the exact solution $\boldsymbol{H}_{\text{ex}}$ so it can be considered as an error estimator of the truncation error. We can see also that this term can be easily calculated from the current i_{2N+1} and the inductance L_{2N+1}which are determined at the stage N of the CLN construction. Similarly, we can obtain couples $(\boldsymbol{H}'^N, \boldsymbol{E}^N)$ and $(\boldsymbol{H}'^N, \boldsymbol{E}'^N)$ satisfying respectively (2) and (1) for the Cauer circuit with an inductive termination, and the error estimator is given by:

$$\begin{aligned} \epsilon_e^2 &= \|\boldsymbol{E}'^N - \boldsymbol{E}^N\|_\sigma^2 \\ &= \|\boldsymbol{E}'^N - \boldsymbol{E}_{\text{ex}}\|_\sigma^2 + \|\boldsymbol{E}_{\text{ex}} - \boldsymbol{E}^N\|_\sigma^2 \\ &= |v_{2N+2}|^2/R_{2N+2} \geq \|\boldsymbol{E}_{\text{ex}} - \boldsymbol{E}^N\|_\sigma^2, \end{aligned} \tag{8}$$

with $\boldsymbol{E}'^N = \boldsymbol{E}^N + v_{2N+2}\boldsymbol{E}_{2N+2}$, and $v_{2N+2} = j\omega L_{2N+1} i_{2N+1}$. The error estimator ϵ_e^2 gives an upper bound of the term $\|\boldsymbol{E}_{\text{ex}} - \boldsymbol{E}^N\|_\sigma^2$.

C. *Upper and lower bounds of energy*

Using the triangular inequality, we obtain:

$$\left| \|\boldsymbol{H}_{\text{ex}}\|_\mu - \left\|\frac{\boldsymbol{H}' + \boldsymbol{H}}{2}\right\|_\mu \right| \leq \left\|\boldsymbol{H}_{\text{ex}} - \frac{\boldsymbol{H}' + \boldsymbol{H}}{2}\right\|_\mu. \tag{9}$$

Based on the property shown in the appendix A, we can show that:

$$\begin{aligned} &\left\|\boldsymbol{H}_{\text{ex}} - \frac{\boldsymbol{H}' + \boldsymbol{H}}{2}\right\|_\mu^2 = \frac{1}{4}\|(\boldsymbol{H}_{\text{ex}} - \boldsymbol{H}') + (\boldsymbol{H}_{\text{ex}} - \boldsymbol{H})\|_\mu^2 \\ &= \frac{1}{4}\left(\|\boldsymbol{H}_{\text{ex}} - \boldsymbol{H}'\|_\mu^2 + \|\boldsymbol{H}_{\text{ex}} - \boldsymbol{H}\|_\mu^2\right) \\ &+ \frac{1}{4}\int_\Omega (\boldsymbol{H}_{\text{ex}} - \boldsymbol{H}') \cdot \mu(\boldsymbol{H}_{\text{ex}} - \boldsymbol{H})^* d\Omega \\ &+ \frac{1}{4}\int_\Omega (\boldsymbol{H}_{\text{ex}} - \boldsymbol{H}) \cdot \mu(\boldsymbol{H}_{\text{ex}} - \boldsymbol{H}')^* d\Omega \\ &= \frac{1}{4}\left(\|\boldsymbol{H}_{\text{ex}} - \boldsymbol{H}'\|_\mu^2 + \|\boldsymbol{H}_{\text{ex}} - \boldsymbol{H}\|_\mu^2\right) = \frac{\epsilon_h^2}{4}. \end{aligned} \tag{10}$$

Combining (9) and (10) results in

$$\left| \|\boldsymbol{H}_{\text{ex}}\|_\mu - \left\|\frac{\boldsymbol{H}' + \boldsymbol{H}}{2}\right\|_\mu \right| \leq \frac{\epsilon_h}{2}, \tag{11}$$

which gives the upper and lower bounds of the exact magnetic energy. When the magnetic fields $\boldsymbol{H}, \boldsymbol{H}'$ are obtained by the CLN method, we can evaluate the term $\left\|\frac{\boldsymbol{H}'+\boldsymbol{H}}{2}\right\|_\mu$ as follows:

$$\begin{aligned} \left\|\frac{\boldsymbol{H}'^N + \boldsymbol{H}^N}{2}\right\|_\mu^2 &= \left\|\boldsymbol{H}^N + \frac{1}{2}i_{2N+1}\boldsymbol{H}_{2N+1}\right\|_\mu^2 \\ &= \|\boldsymbol{H}^N\|_\mu^2 + \left\|\frac{1}{2}i_{2N+1}\boldsymbol{H}_{2N+1}\right\|_\mu^2 \\ &+ \int_\Omega \boldsymbol{H}^N \cdot \mu\left(\frac{1}{2}i_{2N+1}\boldsymbol{H}_{2N+1}\right)^* d\Omega \\ &+ \int_\Omega \left(\frac{1}{2}i_{2N+1}\boldsymbol{H}_{2N+1}\right) \cdot \mu\boldsymbol{H}^{N^*} d\Omega \\ &= \|\boldsymbol{H}^N\|_\mu^2 + \frac{1}{4}L_{2N+1}|i_{2N+1}|^2 \\ &= \|\boldsymbol{H}^N\|_\mu^2 + \left(\frac{\epsilon_h}{2}\right)^2. \end{aligned} \tag{12}$$

Therefore, we can bound the exact value of $\|\boldsymbol{H}_{\text{ex}}\|_\mu$ as follows:

$$d_h - \frac{\epsilon_h}{2} \leq \|\boldsymbol{H}_{\text{ex}}\|_\mu \leq d_h + \frac{\epsilon_h}{2}, \tag{13}$$

with $d_h = \sqrt{\|\boldsymbol{H}^N\|_\mu^2 + (\epsilon_h/2)^2}$. Likewise, we can show that:

$$d_e - \frac{\epsilon_e}{2} \leq \|\boldsymbol{E}_{\text{ex}}\|_\sigma \leq d_e + \frac{\epsilon_e}{2}, \tag{14}$$

with $d_e = \sqrt{\|\boldsymbol{E}^N\|_\sigma^2 + (\epsilon_e/2)^2}$. It is convenient to consider the geometrical relationships of the equations given above. The relationship of the approximations obtained by the CLN method is illustrated in Fig. 2.

III. Numerical Results

A. *Analytical copper foil model*

Let us consider an infinitely long copper foil of thickness $2d$, to which a uniform sinusoidal electric field of magnitude $E_0 = 1$ V/m is applied. We fix $\sigma = 10^7$ [S/m], $\mu = 4\pi \times 10^{-7}$ [H/m] and $d = 0.01$ [m]. The Cartesian coordinate system (x, y, z) is introduced so that the foil has infinite dimensions along y- and z-axes and the source term E_0 is parallel to z-axis. The non-null components of $\boldsymbol{E}_{\text{ex}}$ and $\boldsymbol{H}_{\text{ex}}$ along the z and y axes respectively, are given by [3]:

$$E_{\text{ex}}^z(x) = \frac{\cos(kx)}{\cos(kd)}, \qquad H_{\text{ex}}^y = \frac{k}{j\omega\mu}\frac{\sin(kx)}{\cos(kd)}, \tag{15}$$

with $k = \sqrt{-j\omega\sigma\mu}$. Using the CLN method, we can obtain an analytical expression for the resistance R_{2n} and the inductance L_{2n+1} of the Cauer circuit (see Fig.1) as well as the components of the fields $\boldsymbol{E}_{2n}$ and $\boldsymbol{H}_{2n+1}$ for $n = 0,1,\ldots,N$:

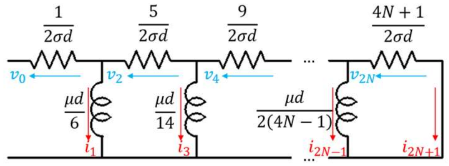

Fig. 1. Cauer circuit with a resistive termination of 1-D foil model.

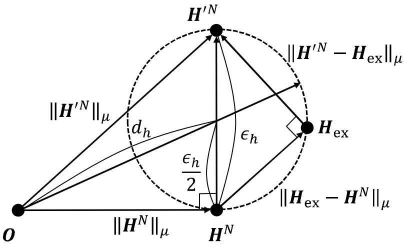

Fig. 2. Geometrical relationship of approximations. The exact solution exists on the circumscribed circle of diameter ϵ_h.

$$E^z_{2n}(x) = P_{2n}\left(\frac{x}{d}\right), \qquad \frac{1}{R_{2n}} = \frac{2\sigma d}{(4n+1)}, \tag{16a}$$

$$H^y_{2n+1}(x) = \frac{1}{2}P_{2n+1}\left(\frac{x}{d}\right), \qquad L_{2n+1} = \frac{\mu d}{2(4n+3)}, \tag{16b}$$

where $P_i\,(x)$ is the i-th Legendre polynomial defined in the interval $[-1,1]$. The electromagnetic fields $\boldsymbol{E}^N$ and $\boldsymbol{H}^N$ are calculated using (5) and (16).

To validate the proposed method and to check (7), we compute the estimator value $\epsilon_h^2{=}L_{2N+1}|i_{2N+1}|^2$ and the term $e_h^2 = \|\boldsymbol{H}'^N - \boldsymbol{H}_{\mathrm{ex}}\|_\mu^2 + \|\boldsymbol{H}_{\mathrm{ex}} - \boldsymbol{H}^N\|_\mu^2$ calculated from the analytical expressions of $\boldsymbol{H}_{\mathrm{ex}}$ in (see (15)) and the analytical expression of $\boldsymbol{H}'^N$ and $\boldsymbol{H}^N$ given by (5) and (16b). In Fig. 3, the evolutions of ϵ_h^2 and e_h^2 as a function of the frequency are presented for different values of N in Fig. 3 (left). We can see first that the error estimator decreases in function of N and also that the relationship (7) is satisfied. We can see also in Fig. 3 (right) that the error estimator is an upper bound of the truncation errors, i.e. the distance between the exact solution $\boldsymbol{H}_{\mathrm{ex}}$ and the magnetic fields $\boldsymbol{H}^N$ or $\boldsymbol{H}'^N$ obtained with the CLN method.

We also compute the estimator value for the electric fields to check (8) for the Cauer circuit with an inductive termination. We can see in Fig. 4 (left) that the relationship (8) is also satisfied. We can see also in Fig.4 (right) the exact value of $\|\boldsymbol{E}_{\mathrm{ex}}\|_\sigma$ belongs to the interval defined by (14).

B. *Inductor FE model*

We apply the proposed method to the FE model of an inductor shown in Fig. 5 (left). We have chosen a mesh sufficiently fine to assume that the error of discretization introduced by the FE method is negligible compared to the truncation error. The FE solution $\boldsymbol{E}_{\mathrm{FE}}$ is assumed to be equal to the exact solution $\boldsymbol{E}_{\mathrm{ex}}$. Now we consider a N-stage Cauer circuit with an inductive termination by applying the CLN method. The error estimator now is based on the calculation of the distance between $\boldsymbol{E}^N$ and $\boldsymbol{E}'^N$. We can compute ϵ_e^2 by (12b) and compare it to the term $e_e^2 = \|\boldsymbol{E}'^N - \boldsymbol{E}_{\mathrm{ex}}\|_\sigma^2 + \|\boldsymbol{E}_{\mathrm{ex}} - \boldsymbol{E}^N\|_\sigma^2$, the fields $\boldsymbol{E}'^N$ and $\boldsymbol{E}^N$ are given by the expansion (5).The values

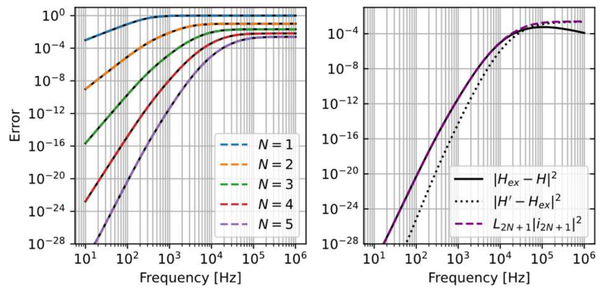

Fig. 3. Comparison of the error estimator ϵ_h^2 (dashed line) and the term $e_h^2 = \|\boldsymbol{H}'^N - \boldsymbol{H}_{\mathrm{ex}}\|_\mu^2 + \|\boldsymbol{H}_{\mathrm{ex}} - \boldsymbol{H}^N\|_\mu^2$ (solid line) as a function of the frequency for different values of N (left). Comparison between the error estimator ϵ_h^2 and the truncation errors $\|\boldsymbol{H}'^N - \boldsymbol{H}_{\mathrm{ex}}\|_\mu^2, \|\boldsymbol{H}_{\mathrm{ex}} - \boldsymbol{H}^N\|_\mu^2$ for N=5 (right).

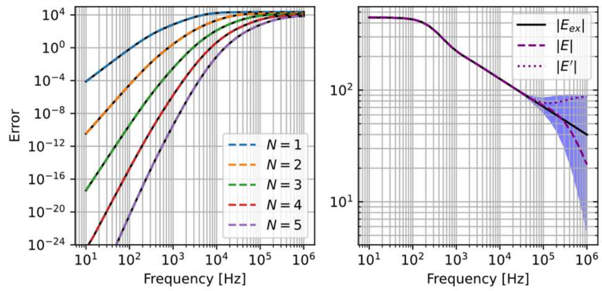

Fig. 4. Comparison of the error estimator ϵ_e^2 (dashed line) and the term $e_e^2 = \|\boldsymbol{E}'^N - \boldsymbol{E}_{\mathrm{ex}}\|_\sigma^2 + \|\boldsymbol{E}_{\mathrm{ex}} - \boldsymbol{E}^N\|_\sigma^2$ (solid line) as a function of the frequency for different values of N (left). Comparison of the values $\|\boldsymbol{E}_{\mathrm{ex}}\|_\sigma$, $\|\boldsymbol{E}^N\|_\sigma$, $\|\boldsymbol{E}'^N\|_\sigma$ for N=5 where the filled area corresponds to the interval given by (13) (right).

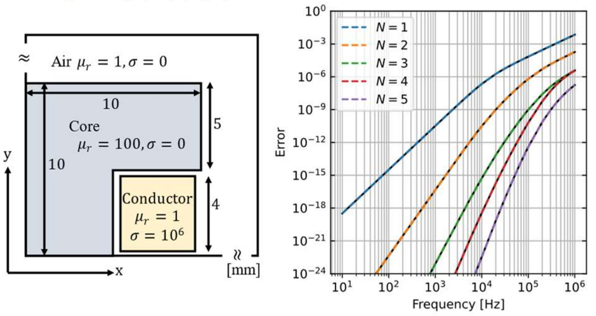

Fig. 5. One-fourth inductor model (left). Comparison of the error estimator $\epsilon_e^2 = |v_{2N+2}|^2/R_{2N+2}$ (dashed line) and the term $e_e^2 = \|\boldsymbol{E}'^N - \boldsymbol{E}_{\mathrm{ex}}\|_\sigma^2 + \|\boldsymbol{E}_{\mathrm{ex}} - \boldsymbol{E}^N\|_\sigma^2$ (solid line) as a function of the frequency for different values of N (right).

ϵ_e^2 and e_e^2 are plotted as a function of the frequency for different values of N in Fig. 5 (right). We can see again in this example that the ϵ_e^2 and e_e^2 are very close verifying that the quantity ϵ_e^2 is an upper bound of the truncation error. We can see also that the truncation error varies a lot with frequency and N so that the estimator can be useful to calibrate N.

IV. Conclusion

In this paper, we have proposed an error estimator which provides guaranteed upper bounds and enables to control the size of the expansion introduced by the CLN method. Analytical and numerical examples have been discussed in order to illustrate the proposed approach. For future perspective, it is significant to consider the discretization error due to the FE approximation [4], error estimation in the timedomain analysis, and CLN with the single or multiple expansion points [5].

Appendix A

Let us consider a triplet $(\boldsymbol{H}, \boldsymbol{H}', \boldsymbol{E})$ such that $(\boldsymbol{H}, \boldsymbol{E})$ and $(\boldsymbol{H}', \boldsymbol{E})$ satisfy (1) and (2), respectively, and the exact solution $(\boldsymbol{H}_{\text{ex}}, \boldsymbol{E}_{\text{ex}})$ to (1) and (2). Firstly, we consider the following equation:

$$\begin{aligned}\epsilon_h^2 &= \|\boldsymbol{H}' - \boldsymbol{H}\|_\mu^2 = \|(\boldsymbol{H}' - \boldsymbol{H}_{\text{ex}}) + (\boldsymbol{H}_{\text{ex}} - \boldsymbol{H})\|_\mu^2 \\ &= \|\boldsymbol{H}' - \boldsymbol{H}_{\text{ex}}\|_\mu^2 + \|\boldsymbol{H}_{\text{ex}} - \boldsymbol{H}\|_\mu^2 \\ &+ \int_\Omega (\boldsymbol{H}' - \boldsymbol{H}_{\text{ex}}) \cdot \mu(\boldsymbol{H}_{\text{ex}} - \boldsymbol{H})^* d\Omega \\ &+ \int_\Omega (\boldsymbol{H}_{\text{ex}} - \boldsymbol{H}) \cdot \mu(\boldsymbol{H}' - \boldsymbol{H}_{\text{ex}})^* d\Omega.\end{aligned} \tag{A1}$$

If we consider now the two inner products in (A1), we have:

$$\begin{aligned}&\int_\Omega (\boldsymbol{H}' - \boldsymbol{H}_{\text{ex}}) \cdot \mu(\boldsymbol{H}_{\text{ex}} - \boldsymbol{H})^* d\Omega \\ &= -\frac{1}{j\omega}\int_\Omega (\boldsymbol{H}' - \boldsymbol{H}_{\text{ex}}) \cdot \text{curl}(\boldsymbol{E}_{\text{ex}} - \boldsymbol{E})^* d\Omega \\ &= -\frac{1}{j\omega}\int_\Omega \text{curl}(\boldsymbol{H}' - \boldsymbol{H}_{\text{ex}}) \cdot (\boldsymbol{E}_{\text{ex}} - \boldsymbol{E})^* d\Omega \\ &+ \frac{1}{j\omega}\int_{\partial\Omega} (\boldsymbol{H}' - \boldsymbol{H}_{\text{ex}}) \times (\boldsymbol{E}_{\text{ex}} - \boldsymbol{E})^* \cdot \boldsymbol{n} d\Gamma \\ &= -\frac{1}{j\omega}\|\boldsymbol{E}_{\text{ex}} - \boldsymbol{E}\|_\sigma^2.\end{aligned} \tag{A2}$$

The boundary integral term $\frac{1}{j\omega}\int_{\partial\Omega}(\boldsymbol{H}' - \boldsymbol{H}_{\text{ex}}) \times (\boldsymbol{E}_{\text{ex}} - \boldsymbol{E})^* \cdot \boldsymbol{n} d\Gamma$ in (A2) vanishes due to the boundary conditions. In the same way, we can show that:

$$\int_\Omega (\boldsymbol{H}_{\text{ex}} - \boldsymbol{H}) \cdot \mu(\boldsymbol{H}' - \boldsymbol{H}_{\text{ex}})^* d\Omega = \frac{1}{j\omega}\|\boldsymbol{E}_{\text{ex}} - \boldsymbol{E}\|_\sigma^2. \tag{A3}$$

Therefore, the two inner products are conjugate pure imaginary numbers and the sum is equal to zero leading to (3). Similarly, we obtain the error estimator (4) for the electric fields to consider a triplet $(\boldsymbol{H}, \boldsymbol{E}, \boldsymbol{E}')$ such that $(\boldsymbol{H}, \boldsymbol{E})$ and $(\boldsymbol{H}, \boldsymbol{E}')$ satisfy (2) and (1), respectively.

Appendix B

Let us consider a N-stage Cauer circuit with a resistive termination, the voltages $v_0, v_2, \ldots, v_{2N}$ and the currents $i_1, i_3, \ldots, i_{2N+1}$ satisfy the circuit equations as follows:

$$\sum_{i=n}^{N} v_{2i} = j\omega L_{2n-1} i_{2n-1}, \qquad n = 1, \cdots, N, \tag{B1}$$

$$\sum_{i=n}^{N} i_{2i+1} = \frac{v_{2n}}{R_{2n}}, \qquad n = 0, \cdots, N. \tag{B2}$$

In addition, the basis obtained by the CLN method satisfies the following relations:

$$\begin{aligned}\text{curl}\boldsymbol{E}_{2n} &= \text{curl}\boldsymbol{E}_{2n-2} - \frac{\mu}{L_{2n-1}}\boldsymbol{H}_{2n-1} \\ &= \sum_{i=0}^{n-1} -\frac{\mu}{L_{2i+1}}\boldsymbol{H}_{2i+1}, \qquad n = 1, \cdots, N,\end{aligned} \tag{B3}$$

$$\begin{aligned}\text{curl}\boldsymbol{H}_{2n+1} &= \text{curl}\boldsymbol{H}_{2n-1} + R_{2n}\sigma\boldsymbol{E}_{2n} \\ &= \sum_{i=0}^{n} R_{2i}\boldsymbol{E}_{2i}, \qquad n = 0, \cdots, N,\end{aligned} \tag{B4}$$

with $\text{curl}\boldsymbol{E}_0 = \boldsymbol{0}$ and $\boldsymbol{H}_{-1} = \boldsymbol{0}$. We can show that $(\boldsymbol{H}^N, \boldsymbol{E}^N)$ and $(\boldsymbol{H}'^N, \boldsymbol{E}^N)$ given by (5), (6) satisfy (1) and (2), respectively:

$$\begin{aligned}\text{curl}\boldsymbol{E}^N &= v_0\text{curl}\boldsymbol{E}_0 + \sum_{n=1}^{N} v_{2n}\text{curl}\boldsymbol{E}_{2n} \\ &= \sum_{n=1}^{N} v_{2n}\left(\sum_{i=0}^{n-1} -\frac{\mu}{L_{2i+1}}\boldsymbol{H}_{2i+1}\right) \\ &= \sum_{i=0}^{N-1} -\frac{\mu}{L_{2i+1}}\boldsymbol{H}_{2i+1}\left(\sum_{n=i+1}^{N} v_{2n}\right) \\ &= \sum_{i=0}^{N-1} -\frac{\mu}{L_{2i+1}}\boldsymbol{H}_{2i+1}(j\omega L_{2i+1} i_{2i+1}) \\ &= -j\omega\mu\boldsymbol{H}^N,\end{aligned} \tag{B5}$$

$$\begin{aligned}\text{curl}\boldsymbol{H}'^N &= \sum_{n=0}^{N} i_{2n+1}\text{curl}\boldsymbol{H}_{2i+1} \\ &= \sum_{n=0}^{N} i_{2n+1}\left(\sum_{i=0}^{n} R_{2i}\sigma\boldsymbol{E}_{2i}\right) \\ &= \sum_{i=0}^{N} R_{2i}\sigma\boldsymbol{E}_{2i}\left(\sum_{n=i}^{N} i_{2n+1}\right) \\ &= \sum_{i=0}^{N} R_{2i}\sigma\boldsymbol{E}_{2i}\left(\frac{v_{2i}}{R_{2i}}\right) = \sigma\boldsymbol{E}^N.\end{aligned} \tag{B6}$$

The third lines in (B5), (B6) can be obtained by considering the order of the variables such as $0 \le i < n \le N$. For a N-stage Cauer circuit with an inductive termination, we consider a triplet $(\boldsymbol{H}'^N, \boldsymbol{E}^N, \boldsymbol{E}'^N)$. We can show that $(\boldsymbol{H}'^N, \boldsymbol{E}^N)$ and $(\boldsymbol{H}'^N, \boldsymbol{E}'^N)$ satisfy (2) and (1), respectively. The proof for (2) is the same as (B6). The voltages satisfy the equations as follows:

$$\sum_{i=n}^{N+1} v_{2i} = j\omega L_{2n-1} i_{2n-1}, \qquad n = 1, \cdots, N, \tag{B7}$$

with $v_{2N+2} = j\omega L_{2N+1} i_{2N+1}$. Using (B7), we can show (1) for $(\boldsymbol{H}'^N, \boldsymbol{E}'^N)$ in the same way as (B5).

References

[1] A. Kameari, H. Ebrahimi, K. Sugahara, Y. Shindo, and T. Matsuo, “Cauer Ladder Network Representation of Eddy-Current Fields for Model Order Reduction Using Finite-Element Method,” *IEEE Trans. Magn.*, vol. 54, no. 3, pp. 1–4, Mar. 2018.

[2] Z. Tang, Y. Le Menach, E. Creusé, S. Nicaise, F. Piriou and N. Nemitz, "Residual and Equilibrated Error Estimators for Magnetostatic Problems Solved by Finite Element Method," *IEEE Trans. Magn.*, vol. 49, no. 12, pp. 5715-5723, Dec. 2013.

[3] J. Lammeraner and M. Stafl, “Eddy Currents,” London, U.K.: ILIFFE Books, pp.15-18, 1966.

[4] S. Hiruma and H. Igarashi, “Model Order Reduction for Linear Time-Invariant System With Symmetric Positive-Definite Matrices: Synthesis of Cauer-Equivalent Circuit,” *IEEE Trans. Magn.*, vol. 56, no. 3, pp. 1–8, Mar. 2020.

[5] K. Kuriyama et al., “Cauer Ladder Network With Multiple Expansion Points for Efficient Model Order Reduction of Eddy-Current Field,” *IEEE Trans. Magn.*, vol. 55, no. 6, pp. 1–4, Jun. 2019.